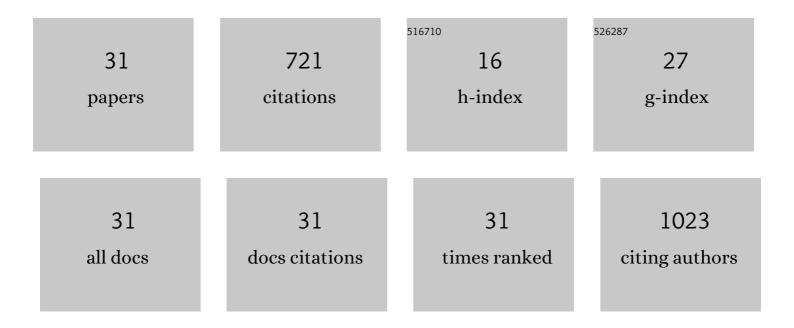
Juan Tang

List of Publications by Year in descending order

Source: https://exaly.com/author-pdf/4845480/publications.pdf Version: 2024-02-01



ΙΠΑΝ ΤΑΝΟ

#	Article	IF	CITATIONS
1	Biocatalysis-mediated MOF-to-prussian blue transformation enabling sensitive detection of NSCLC-associated miRNAs with dual-readout signals. Biosensors and Bioelectronics, 2022, 206, 114139.	10.1	28
2	Direct C–H Sulfonylimination of Pyridinium Salts. Organic Letters, 2022, 24, 2821-2825.	4.6	10
3	Visibleâ€Lightâ€Enabled Photosensitizer―and Additiveâ€Free Decarboxylative Coupling Cyclization of Enaminone with <i>N</i> â€Arylglycine for 3â€Aminoalkyl Chromones. Advanced Synthesis and Catalysis, 2022, 364, 2169-2173.	4.3	11
4	Facile Synthesis of 2-Methylnicotinonitrile through Degenerate Ring Transformation of Pyridinium Salts. Journal of Organic Chemistry, 2022, 87, 7975-7988.	3.2	3
5	lodination/Amidation of the <i>N</i> -Alkyl (Iso)quinolinium Salts. Journal of Organic Chemistry, 2021, 86, 716-730.	3.2	8
6	A portable thermal detection method based on the target responsive hydrogel mediated self-heating of a warming pad. Chemical Communications, 2021, 57, 9862-9865.	4.1	6
7	Copper-catalyzed oxidative cyclization of glycine derivatives toward 2-substituted benzoxazoles. Organic and Biomolecular Chemistry, 2021, 19, 1616-1619.	2.8	5
8	Visibleâ€Lightâ€Induced Aerobic Oxidative C <i>sp</i> ³ â^'H Functionalization of Glycine Derivatives for 2â€6ubstituted Benzoxazoles. Advanced Synthesis and Catalysis, 2021, 363, 2568-2572.	4.3	14
9	Ultrasensitive zero-background photoelectrochemical biosensor for analysis of organophosphorus pesticide based on in situ formation of DNA-templated Ag2S photoactive materials. Analytical and Bioanalytical Chemistry, 2021, 413, 6279-6288.	3.7	11
10	Asymmetric synthesis of chiral organosilicon compounds <i>via</i> transition metal-catalyzed stereoselective C–H activation and silylation. Chemical Communications, 2021, 57, 8250-8263.	4.1	33
11	Highly Efficient Copper-Catalyzed Dehydrogenative Cross-Coupling of Azoles with α-Amino Carbonyl Compounds. Synthesis, 2021, 53, 2277-2285.	2.3	1
12	Palladium-Catalyzed Direct Arylation of Alkylpyridine via Activated <i>N</i> -Methylpyridinium Salts. Journal of Organic Chemistry, 2020, 85, 622-632.	3.2	7
13	Rolling circle amplification promoted magneto-controlled photoelectrochemical biosensor for organophosphorus pesticides based on dissolution of core-shell MnO2 nanoflower@CdS mediated by butyrylcholinesterase. Mikrochimica Acta, 2020, 187, 450.	5.0	26
14	Ultrasensitive split-type electrochemical sensing platform for sensitive determination of organophosphorus pesticides based on MnO2 nanoflower-electron mediator as a signal transduction system. Analytical and Bioanalytical Chemistry, 2020, 412, 6939-6945.	3.7	22
15	Visible-Light-Induced Dehydrogenative Imidoylation of Imidazo[1,2- <i>a</i>]pyridines with α-Amino Acid Derivatives and α-Amino Ketones. Journal of Organic Chemistry, 2020, 85, 15062-15071.	3.2	15
16	Target-induced elimination of photosensitizer and formation insulation layer enabling ultrasensitive photoelectrochemical detection of ochratoxin A. Sensors and Actuators B: Chemical, 2019, 297, 126707.	7.8	21
17	Target-engineered photo-responsive DNA strands: a novel signal-on photoelectrochemical biosensing platform for ochratoxin A. Analytical Methods, 2019, 11, 5638-5644.	2.7	11
18	Enzymatic oxydate-triggered AgNPs etching: A novel signal-on photoelectrochemical immunosensing platform based on Ag@AgCl nanocubes loaded RGO plasmonic heterostructure. Biosensors and Bioelectronics, 2019, 130, 125-131.	10.1	41

Juan Tang

#	Article	IF	CITATIONS
19	Photocatalyst-free decarboxylative aminoalkylation of imidazo[1,2- <i>a</i>]pyridines with <i>N</i> -aryl glycines enabled by visible light. Organic Chemistry Frontiers, 2019, 6, 3693-3697.	4.5	35
20	Two-dimensional MoS2 as a nano-binder for ssDNA: Ultrasensitive aptamer based amperometric detection of Ochratoxin A. Mikrochimica Acta, 2018, 185, 162.	5.0	39
21	A conventional chemical reaction for use in an unconventional assay: A colorimetric immunoassay for aflatoxin B1 by using enzyme-responsive just-in-time generation of a MnO2 based nanocatalyst. Mikrochimica Acta, 2018, 185, 92.	5.0	32
22	Effect of combining adsorption-stripping treatment with acidification on the growth of Chlorella vulgaris and nutrient removal from swine wastewater. Bioresource Technology, 2018, 263, 10-16.	9.6	49
23	Nonenzymatic sensing of hydrogen peroxide using a glassy carbon electrode modified with graphene oxide, a polyamidoamine dendrimer, and with polyaniline deposited by the Fenton reaction. Mikrochimica Acta, 2018, 185, 569.	5.0	16
24	In-situ amplified voltammetric immunoassay for ochratoxin A by couplingÂa platinum nanocatalyst based enhancement to a redox cycling process promoted by an enzyme mimicÂ. Mikrochimica Acta, 2017, 184, 2445-2453.	5.0	26
25	DNA-based electrochemical determination of mercury(II) by exploiting the catalytic formation of gold amalgam and of silver nanoparticles. Mikrochimica Acta, 2016, 183, 1805-1812.	5.0	22
26	Amplified impedimetric immunosensor based on instant catalyst for sensitive determination of ochratoxin A. Biosensors and Bioelectronics, 2016, 86, 386-392.	10.1	42
27	Novel glucometer-based immunosensing strategy suitable for complex systems with signal amplification using surfactant-responsive cargo release from glucose-encapsulated liposome nanocarriers. Biosensors and Bioelectronics, 2016, 79, 508-514.	10.1	43
28	Homogeneous electrochemical immunoassay of aflatoxin B1 in foodstuff using proximity-hybridization-induced omega-like DNA junctions and exonuclease III-triggered isothermal cycling signal amplification. Analytical and Bioanalytical Chemistry, 2016, 408, 8593-8601.	3.7	15
29	A Green Strategy to Prepare Metal Oxide Superstructure from Metal-Organic Frameworks. Scientific Reports, 2015, 5, 8401.	3.3	54
30	Non-enzymatic electrochemical immunoassay using noble metal nanoparticles: a review. Mikrochimica Acta, 2015, 182, 2077-2089.	5.0	74
31	The model of generalized partially horizontal collaborative fuzzy C-means. , 2009, , .		1